Broadening Mn^{2+}/Mn^{3+} redox platform in $LiMn_{0.6}Fe_{0.4}PO_4$ cathodes for high-power and long-life Li-ion batteries

Pengxu Wang[1], Yaoguo Fang[2], Erdong Zhang[2], Ling Chen[1], Haifeng Yu[1]*, Qian Cheng[2]*, Hao Jiang[1]*

[1] *Key Laboratory for Ultrafine Materials of Ministry of Education, School of Materials Science and Engineering, East China University of Science and Technology, Shanghai 200237, China*

[2] *Shanghai Xuanyi New Energy Development Co., Ltd, Shanghai 201800, China*

*Corresponding authors

E-mail address: hfyu@ecust.educ.cn (Dr. H. F. Yu), q.cheng@gotion.com (Dr. Q. Cheng), and jianghao@ecust.edu.cn (Prof. H. Jiang)

Tel.: +86-21-64250949; Fax: +86-21-64250624.

Part I Supporting Figures

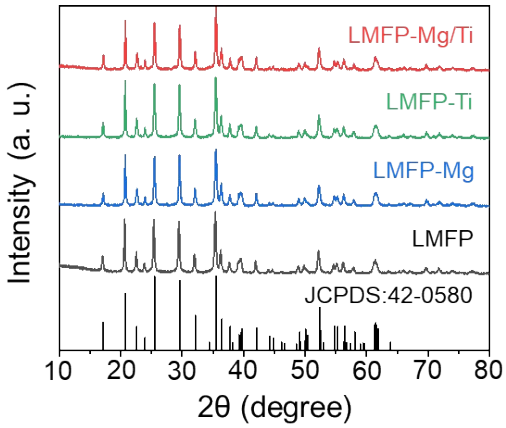

Fig. S1 XRD patterns of LMFP, LMFP-Mg, LMFP-Ti, and LMFP-Mg/Ti.

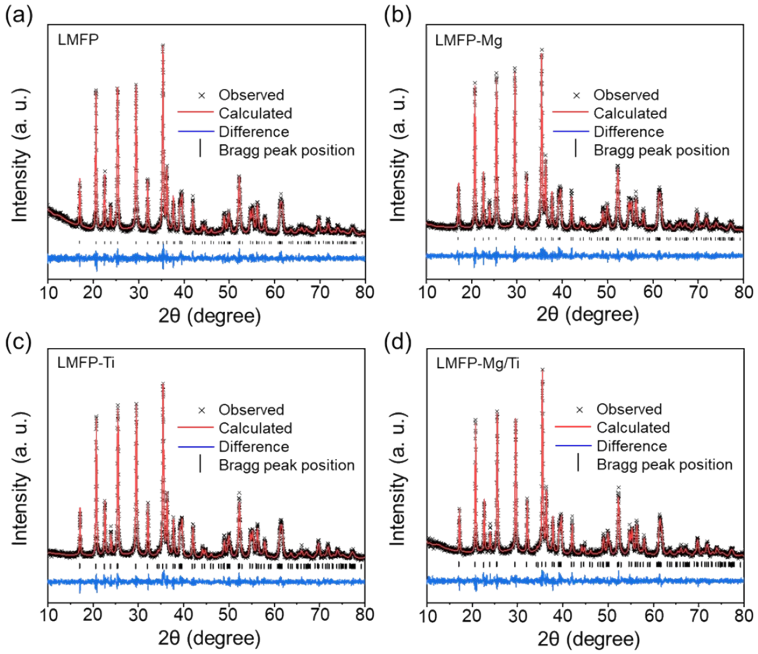

Fig. S2 XRD refinement results of LMFP, LMFP-Mg, LMFP-Ti, and LMFP-Mg/Ti.

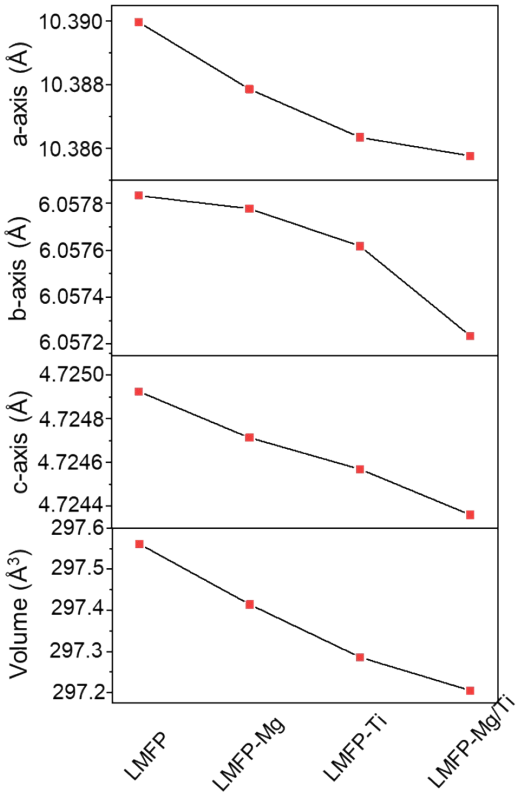

Fig. S3 Refined cell parameters of both a, b, c, and v for LMFP, LMFP-Mg, LMFP-Ti, and LMFP-Mg/Ti.

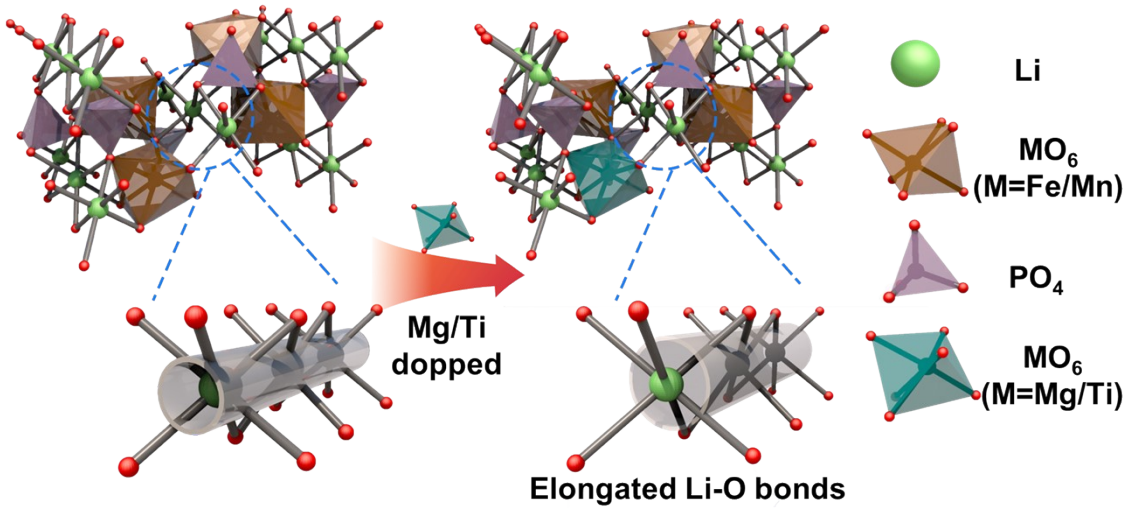

Fig. S4 The structural diagram of the elongation of the Li-O bonds.

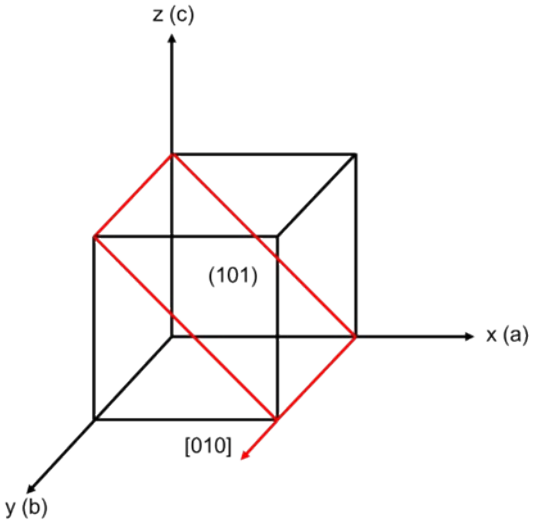

Fig. S5 The schematic of crystal plane.

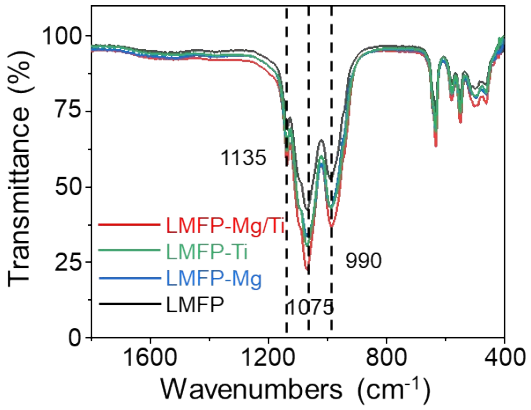

Fig. S6 The FT-IR spectroscopy of LMFP, LMFP-Mg, LMFP-Ti and LMFP-Mg/Ti.

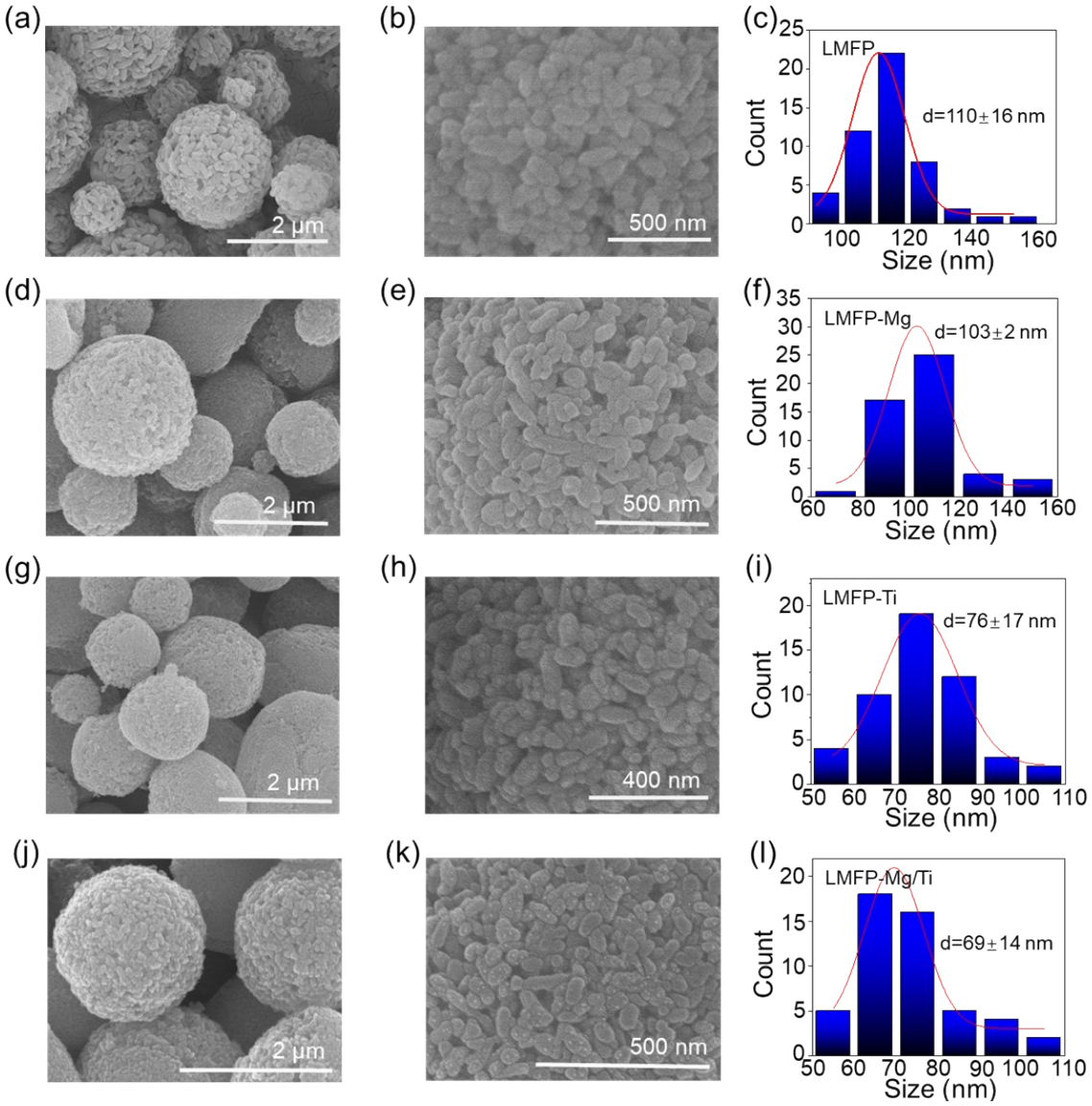

Fig. S7 The SEM images of (a, b, c) LMFP, (d, e, f) LMFP-Mg, (g, h, i) LMFP-Ti, and (j, k, l) LMFP-Mg/Ti at different resolutions and their particle size analysis.

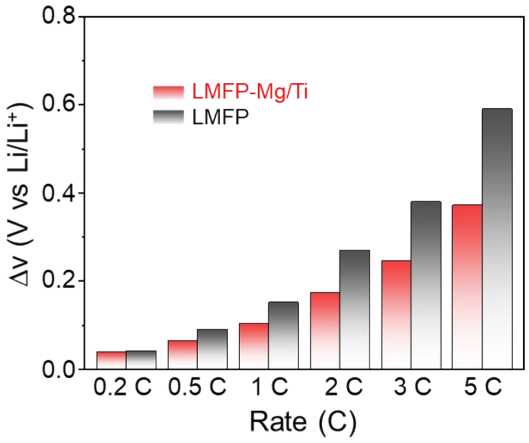

Fig. S8 Overpotential of Mn plateau for LFMP and LMFP-Mg/Ti at different current rates.

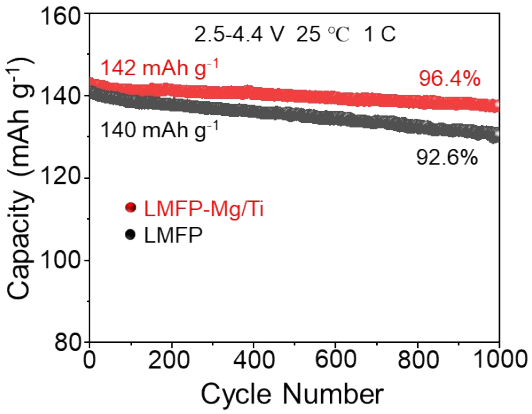

Fig. S9 The cycle performance of LMFP and LMFP-Mg/Ti at 1 C.

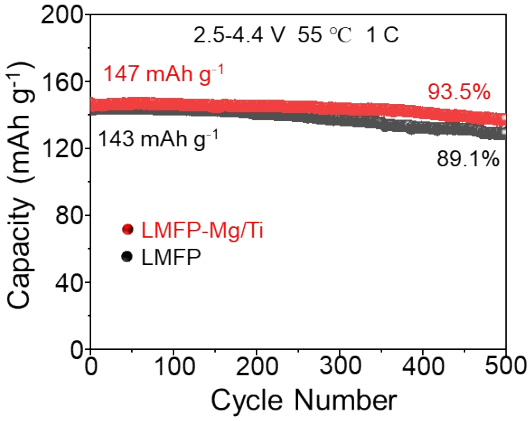

Fig. S10 The cycle performance of LMFP and LMFP-Mg/Ti at 55 ℃.

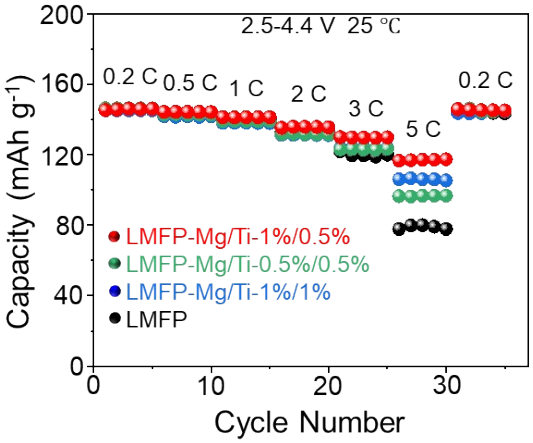

Fig. S11 The rate performance of cathode with different Mg^{2+} and Ti^{4+} contents.

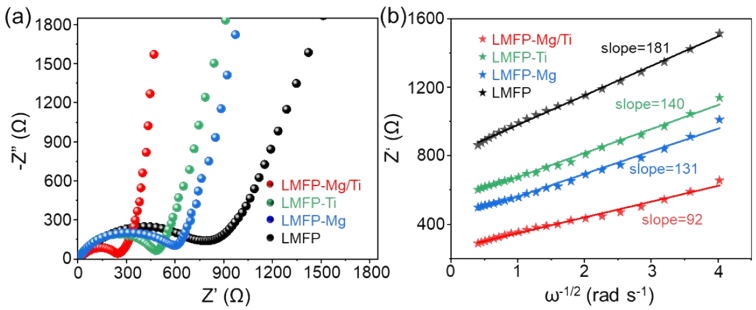

Fig. S12 The linear relationship of Z' versus $\omega^{-1/2}$ in the low-frequency region for LFMP, LMFP-Mg, LMFP-Ti, and LMFP-Mg/Ti.

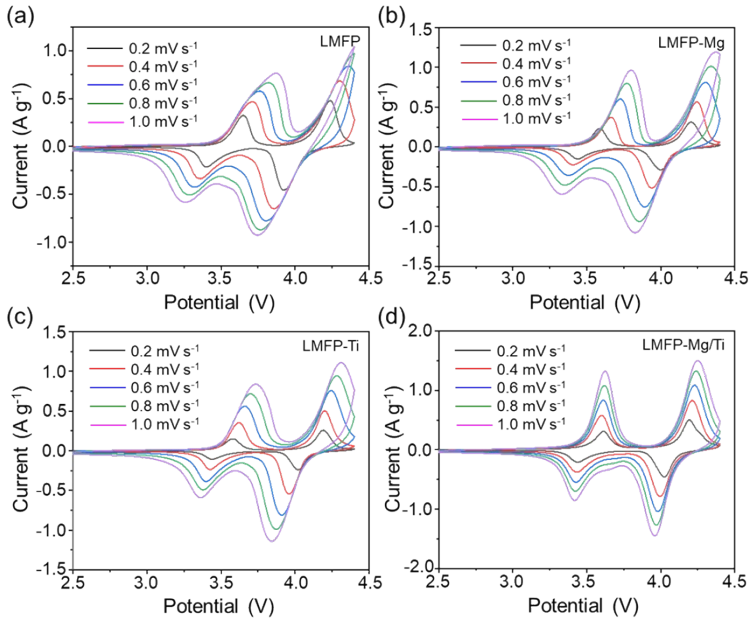

Fig. S13 CV curves of (a) LMFP, (b) LMFP-Mg, (c) LMFP-Ti, and (d) LMFP-Mg/Ti at various sweep rates from 0.2 to 1.0 $mV \cdot s^{-1}$ in 2.5-4.4 V.

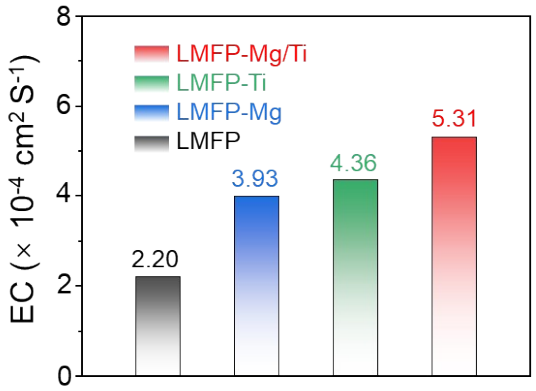

Fig. S14 Electronic conductivity of the LMFP, LMFP-Mg, LMFP-Ti and LMFP-Mg/Ti.

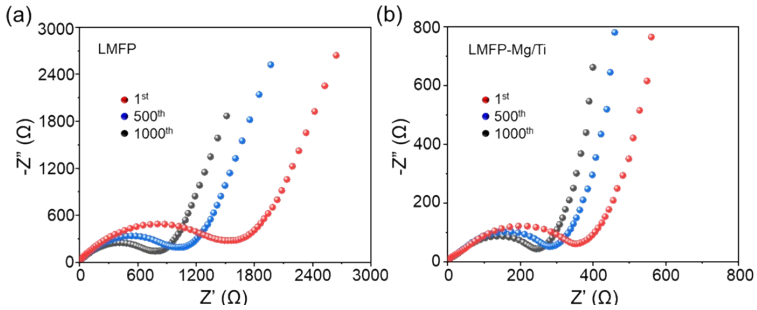

Fig. S15 Nyquist curves of (a) LMFP and (b) LMFP-Mg/Ti before and after cycling.

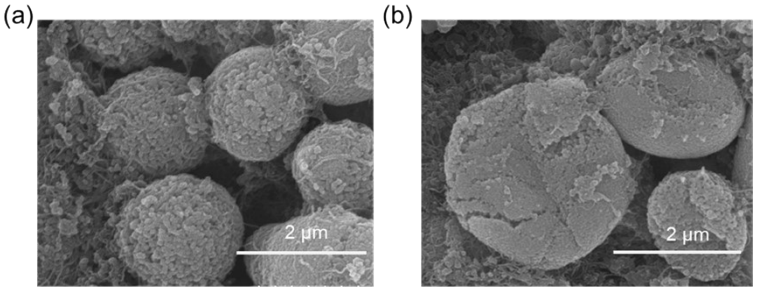

Fig. S16 SEM images of (a) LMFP-Mg/Ti and (b) LMFP after 1000 cycles at 3 C.

Part II: Supporting Tables

Table S1 Lattice parameters obtained from XRD Rietveld refinements.

Samples	a	b	c	v	R_{wp}%
LMFP	10.38997	6.05783	4.72492	297.561	8.01
LMFP-Mg	10.38786	6.05778	4.72471	297.414	7.82
LMFP-Ti	10.38635	6.05762	4.72457	297.286	7.56
LMFP-Mg/Ti	10.38576	6.05723	4.72436	297.205	7.54

Table S2 ICP results for LMFP-Co/Na.

Elements	Mn	Fe	Mg	Ti
LMFP-Mg/Ti	59.1%	39.3%	0.98%	0.47%

Table S3 Electrochemical performance and cycle stability of LMFP cathodes reported in the literature.

Samples	Voltage(V)	Cycle performance	Reference
LMFP-Mg/Ti	2.5-4.4 V	94.6% (3 C, 1000 cycles)	This work
LMFP-700 ℃	2.5-4.4V	91.1% (0.5 C 300 cycles)	1
LMFP/C-Fe	2.0-4.5	93.8% (0.5 C 300 cycles)	2
Mg/Ni-LMFP/C	2.5-4.3 V	95% (1 C 1000 cycles)	3
LMFP-2	2.0-4.5 V	93.7% (1 C 300 cycles)	4
LMFP-BASE-9	2.5-4.2 V	92.9% (0.5 C 200 cycles)	5
LMFP/C	2.0-4.5 V	81.7% (0.1 C 100 cycles)	6
LFMP-0.75%LiBOB	2.5-4.5 V	95.3% (1 C 200 cycles)	7
LFMP/C+R-LCO	2.7-4.3 V	95.2% (1 C 100 cycles)	8

Reference

[1] J. Liu, Y. Wu, B. Zhang, X. Xiao, Q. Hu, Q. Han, L. Wang, F. Bei and X. He, Small, 2023, 2309629.

[2] H. Hu, X. Liu, Y. Lei, J. Chen, L. Wu, Z. Li, J. Liu and X. Wang, J. Energy Storage, 2024, **79**, 110198.

[3] H. Yu, E. Zhang, J. Yu, S. Yu, Y. Fang, L. Chen, H. Jiang and C. Li, J. Mater. Chem. A, 2024, **12**, 26076-26082.

[4] B. Zhang, W. Meng, Y. Gong, G. Hu, Z. Peng, K. Du, B. Makuza, J. Wu, X. Xie and Y. Cao, Mater. Today Energy, 2022, **30**, 101162.

[5] M. Yao, H. Zhang, C. Xing, Q. Li, Y. Tang, F. Zhang, K. Yang and S. Zhang, Energy Storage Mater., 2021, **41**, 51-60.

[6] S. Wi, J. Park, S. Lee, J, Kang, T. Hwang, K. Lee, H. Lee, S. Namd, C. Kime, Y. Sung and B. Park, Nano Energy, 2017, **31**, 495-503.

[7] Y. Liu, X. Wen, T. Huang and A. Yu, J. Power Sources, 2024, **623**, 235398.

[8] Y. Wu, J. Ju, B. Shen, J. Wei, H. Jiang, C. Li and Y. Hu, Small, 2024, 2311891.